JCI The Journal of Clinical Investigation

CSF-1 signaling mediates recovery from acute kidney injury

Ming-Zhi Zhang, … , Amar Singh, Raymond C. Harris

Research Article   **Nephrology**

Renal tubule epithelia represent the primary site of damage in acute kidney injury (AKI), a process initiated and propagated by the infiltration of macrophages. Here we investigated the role of resident renal macrophages and dendritic cells in recovery from AKI after ischemia/reperfusion (I/R) injury or a novel diphtheria toxin–induced (DT-induced) model of selective proximal tubule injury in mice. DT-induced AKI was characterized by marked renal proximal tubular cell apoptosis. In both models, macrophage/dendritic cell depletion during the recovery phase increased functional and histologic injury and delayed regeneration. After I/R-induced AKI, there was an early increase in renal macrophages derived from circulating inflammatory (M1) monocytes, followed by accumulation of renal macrophages/dendritic cells with a wound-healing (M2) phenotype. In contrast, DT-induced AKI only generated an increase in M2 cells. In both models, increases in M2 cells resulted largely from in situ proliferation in the kidney. Genetic or pharmacologic inhibition of macrophage colony-stimulating factor (CSF-1) signaling blocked macrophage/dendritic cell proliferation, decreased M2 polarization, and inhibited recovery. These findings demonstrated that CSF-1–mediated expansion and polarization of resident renal macrophages/dendritic cells is an important mechanism mediating renal tubule epithelial regeneration after AKI.

Find the latest version:

https://jci.me/60363/pdf

CSF-1 signaling mediates recovery from acute kidney injury

Ming-Zhi Zhang,[1,2] Bing Yao,[1] Shilin Yang,[1] Li Jiang,[1] Suwan Wang,[1] Xiaofeng Fan,[1] Huiyong Yin,[1] Karlton Wong,[1] Tomoki Miyazawa,[1] Jianchun Chen,[1] Ingrid Chang,[1] Amar Singh,[1] and Raymond C. Harris[1,3,4]

[1]Department of Medicine, [2]Department of Cancer Biology, and [3]Department of Molecular Physiology and Biophysics, Vanderbilt University School of Medicine, Nashville, Tennessee, USA. [4]Nashville Veterans Affairs Hospital, Nashville, Tennessee, USA.

Renal tubule epithelia represent the primary site of damage in acute kidney injury (AKI), a process initiated and propagated by the infiltration of macrophages. Here we investigated the role of resident renal macrophages and dendritic cells in recovery from AKI after ischemia/reperfusion (I/R) injury or a novel diphtheria toxin–induced (DT-induced) model of selective proximal tubule injury in mice. DT-induced AKI was characterized by marked renal proximal tubular cell apoptosis. In both models, macrophage/dendritic cell depletion during the recovery phase increased functional and histologic injury and delayed regeneration. After I/R-induced AKI, there was an early increase in renal macrophages derived from circulating inflammatory (M1) monocytes, followed by accumulation of renal macrophages/dendritic cells with a wound-healing (M2) phenotype. In contrast, DT-induced AKI only generated an increase in M2 cells. In both models, increases in M2 cells resulted largely from in situ proliferation in the kidney. Genetic or pharmacologic inhibition of macrophage colony-stimulating factor (CSF-1) signaling blocked macrophage/dendritic cell proliferation, decreased M2 polarization, and inhibited recovery. These findings demonstrated that CSF-1–mediated expansion and polarization of resident renal macrophages/dendritic cells is an important mechanism mediating renal tubule epithelial regeneration after AKI.

Introduction

Acute kidney injury (AKI) is defined as an abrupt decrease in renal function. The reported incidence of AKI varies from 5% in all hospitalized patients to 30%–50% in intensive care units (1). Although the previous term commonly used for AKI, *acute tubule necrosis*, was something of a misnomer, it is clear that the renal tubule epithelia, and especially cells of the proximal tubule, are the primary targets for injury. Depending on the nature and extent of the injurious stimuli, tubular cells lose functional integrity transiently or die by necrosis or apoptosis. The proximate cause of the epithelial cell injury appears to be multifactorial, whether the etiology of AKI is ischemic, septic, toxic, or some combination thereof. There is increasing evidence that infiltrating cells play an important role in the initiation and propagation of the tubule dysfunction and structural injury (2), and maneuvers that inhibit renal infiltration of neutrophils (3, 4), lymphocytes (5, 6), or macrophages (7–9) lead to decreased tubule damage.

It is currently thought that epithelial cell repair in response to AKI is accomplished primarily by the dedifferentiation, migration, and proliferation of surviving tubular cells, with ultimate restoration of tissue integrity (10, 11). It remains uncertain whether all surviving tubule epithelial cells retain the ability to repopulate the tubule or whether regeneration is accomplished by a subpopulation of still incompletely characterized stem cells endogenous to the kidney (12–14). Also unclear are the factors stimulating the epithelial repair. Administration of exogenous growth factors, such as HGF, IGF-1, and members of the EGF family of growth factors, accelerates recovery (15), and renal expression of these factors does increase in response to AKI (15, 16). Although previous studies had suggested a role for bone marrow–derived

stem cells, more recent investigation has discounted such cells as a major source of progenitor cells. However, administration of mesenchymal stem cells does accelerate repair of damaged renal epithelia through the paracrine effects of secreted growth factors, cytokines, and chemokines (17).

An associated question that has also been incompletely explored to date concerns the role of resident and/or infiltrating hematopoietic cells as mediators of recovery from acute tubule injury. The role of macrophages is of particular interest because they can exhibit distinctly different functional phenotypes, broadly characterized as proinflammatory (M1, or *classically activated*) and tissue-reparative (M2, or *alternatively activated*) phenotypes (18, 19). Resident macrophages and dendritic cells demonstrate significant overlap in surface marker expression with M2 macrophages (20). Distinctly different roles for these monocyte subtypes have been reported in injury and recovery in other organs (21–23), and recent studies have indicated similarly distinct roles in response to ischemia/reperfusion (I/R) injury in the kidney (24, 25). As noted above, preventing the initial influx of macrophages lessens ischemia-induced renal injury, but the design of these studies allowed only minimal determination of the roles of renal macrophages and/or dendritic cells during the recovery phase. We now report a novel model of renal injury induced by administration of diphtheria toxin (DT) to a transgenic mouse expressing the human DT receptor (DTR) selectively in the proximal tubule. In this model of targeted apoptosis of the epithelial cells, there was minimal infiltration from circulating hematopoietic cells. However, in both this model and a model of kidney I/R injury, renal cells of monocytic origin expressing markers of reparative macrophages and dendritic cells were necessary for recovery from injury, and we describe a crucial role for CSF-1 signaling to mediate their in situ proliferation and differentiation in the kidney during the recovery phase after AKI.
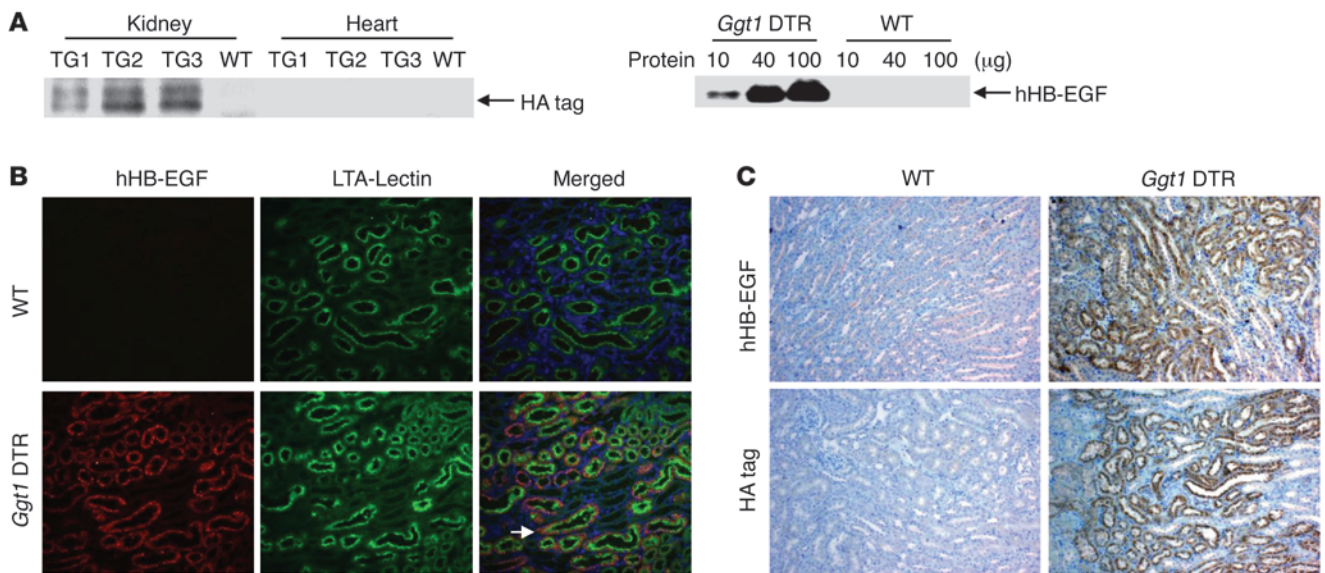
Figure 1
hHB-EGF (DTR) was selectively expressed in renal proximal tubule in *Ggt1* DTR transgenic mice. (**A**) HA-tag was detected only in *Ggt1* DTR (TG) kidneys, not in WT or *Ggt1* DTR hearts. hHB-EGF was detected only in *Ggt1* DTR kidneys. (**B**) Representative photomicrographs showing hHB-EGF colocalization (arrow) with *L. tetragonolobus* lectin (LTA-lectin), a marker of proximal tubule. Original magnification, ×400. (**C**) Representative photomicrographs showing hHB-EGF and HA-tag expression in kidney cortex and outer medulla of *Ggt1* DTR mice, but not WT mice. Original magnification, ×63.

Results

In order to develop a model of selective proximal tubule injury, we transfected the B6D2 strain of mice with a human proHB-EGF (hHB-EGF) cDNA construct linked to the proximal 2,185 bp of the promoter of gamma glutamyl transferase (*Ggt1*), which is selectively expressed in the proximal tubule of the postnatal mammalian kidney (26) and linked at the carboxyl terminal with a HA tag (Supplemental Figure 1A; supplemental material available online with this article; doi:10.1172/JCI60363DS1). We identified 12 founders expressing the transgene and used 3 founders for subsequent characterization. Immunoblotting (Figure 1A) or RT-PCR (Supplemental Figure 1, B and C) for either hHB-EGF or the HA tag indicated selective hHB-EGF expression in kidney, with no expression in heart or liver. Immunofluorescence indicated colocalization of hHB-EGF with the proximal tubule–specific lectin *Lotus tetragonolobus* (Figure 1B); a predominantly proximal tubule localization was confirmed by immunohistochemistry using antibodies against hHB-EGF and HA (Figure 1C).

To determine the response of the transgenic mice to DT, male mice (2–3 months of age) were administered varying concentrations of a single i.p. injection of DT. In WT littermates, a concentration of 10,000 ng/kg DT did not increase BUN or alter histology (Figure 2, A and B), consistent with the lack of binding of DT to murine HB-EGF. In the human hHB-EGF transgenic mice (referred to herein as *Ggt1* DTR mice), DT induced concentration-dependent increases in BUN and creatinine, but the rate of increase was slower than that of I/R (Supplemental Figure 2), with increases not seen until 2 days after injection and peak increases occurring at 5–6 days (Figure 2A and Figure 3D). The alterations in renal function were accompanied by histologic confirmation of proximal tubule injury, with tubule dilation, loss of brush border, sloughing of individual epithelial cells, and distal

cast formation (Figure 2B). DT induced apoptosis in the transgenic mice, with expression of caspase-9 and cleaved caspase-3 increasing within 1 day after administration (Figure 2C). Cleaved caspase-3 immunostaining indicated increased epithelial apoptosis in kidneys 2 days after DT injection (Supplemental Figure 3). Another marker of apoptosis, TUNEL staining, was also found to increase in the kidneys within 2 days after DT administration and to decrease by 5 days (Figure 2D). Evidence of regeneration, indicated by Ki67 staining, was detectable within 2 days after DT administration, with a peak at 8 days and decreased expression by 12 days (Figure 2E). However, albuminuria, as determined by 24-hour urinary albumin excretion, persisted for up to 4 weeks (Supplemental Figure 4), indicative of a delay in complete recovery of proximal tubule function.

After DT administration, there was increased expression of the monocyte/macrophage marker F4/80 (Figure 3A). Flow cytometry indicated that at baseline, 2.44% ± 0.39% of renal cells were F4/80^{hi}. At 5 and 8 days, F4/80^{hi} cells markedly increased to 6.93% ± 2.19% and 13.11% ± 3.23%, respectively, of renal cells (*n* = 4–6; Figure 3B). At 8 days after DT administration, the majority of the cells were CD11b^{hi}F4/80^{hi}CD11c^{+} (58% ± 6%; *n* = 4), while the remainder were CD11b^{hi}F4/80^{hi}CD11c^{-} (35% ± 7%; *n* = 4). There were minimal CD11b^{lo}F4/80^{hi}CD11c^{+} or CD11b^{lo}F4/80^{hi}CD11c^{-} cells. Further flow cytometric analysis indicated that CD11b^{hi}F4/80^{hi}CD11c^{+} cells expressed cell surface markers consistent with dendritic cells (CD11b^{lo}F4/80^{hi}CD11c^{+} IA^{hi}CX3CR1^{+}CD86^{+}), whereas CD11b^{hi}F4/80^{hi}CD11c^{-} cells had a phenotype consistent with tissue macrophages (CD11b^{hi}F4/80^{lo}CD62L^{+}Ly6C^{hi}Gr-1^{int}; Table 1 and ref. 27).

In order to determine their role in the observed injury, macrophages/dendritic cells were depleted by clodronate administration. Clodronate effectively depleted macrophages/dendritic
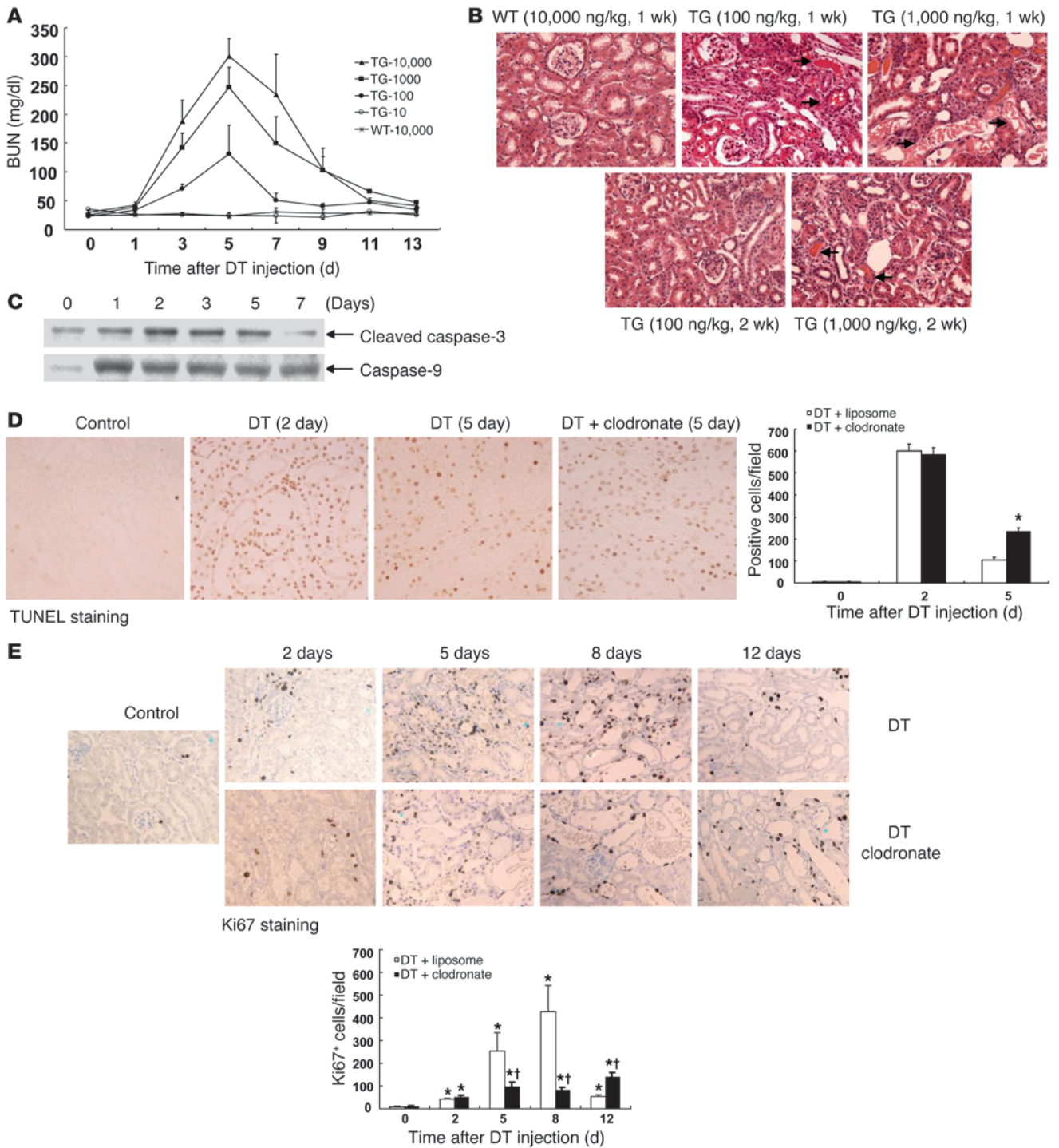
Figure 2

DT induced AKI in *Ggt1* DTR mice. (**A**) DT induced concentration-dependent increases in BUN in *Ggt1* DTR mice ($n = 4$–6). (**B**) Representative histological photomicrographs demonstrating that renal injury (arrows) was more severe in mice 1 week after injection with 1,000 ng/kg DT than with 100 ng/kg DT. After 2 weeks, renal injury was still evident in mice with 1,000 ng/kg, but not 100 ng/kg, DT. Original magnification, ×100. (**C**) DT induced rapid and transient increases in cleaved caspase-3 and caspase-9 expression in *Ggt1* DTR mouse kidney. (**D**) DT induced tubule epithelial apoptosis (TUNEL staining) in *Ggt1* DTR mouse kidney, which peaked at day 2 and was decreased by 5 days after administration. Recovery from DT-mediated apoptosis was attenuated by macrophage/dendritic cell depletion with clodronate (*$P < 0.01$ vs. DT plus liposome at 5 days; $n = 3$ per group). Original magnification, ×250. (**E**) The number of Ki67+ cells increased by 2 days after DT administration and peaked 5–8 days after DT injection. Proliferation was significantly attenuated by macrophage/dendritic cell depletion (*$P < 0.01$ vs. baseline; †$P < 0.01$ vs. corresponding DT plus liposome; $n = 4$ per group). Original magnification, ×250.
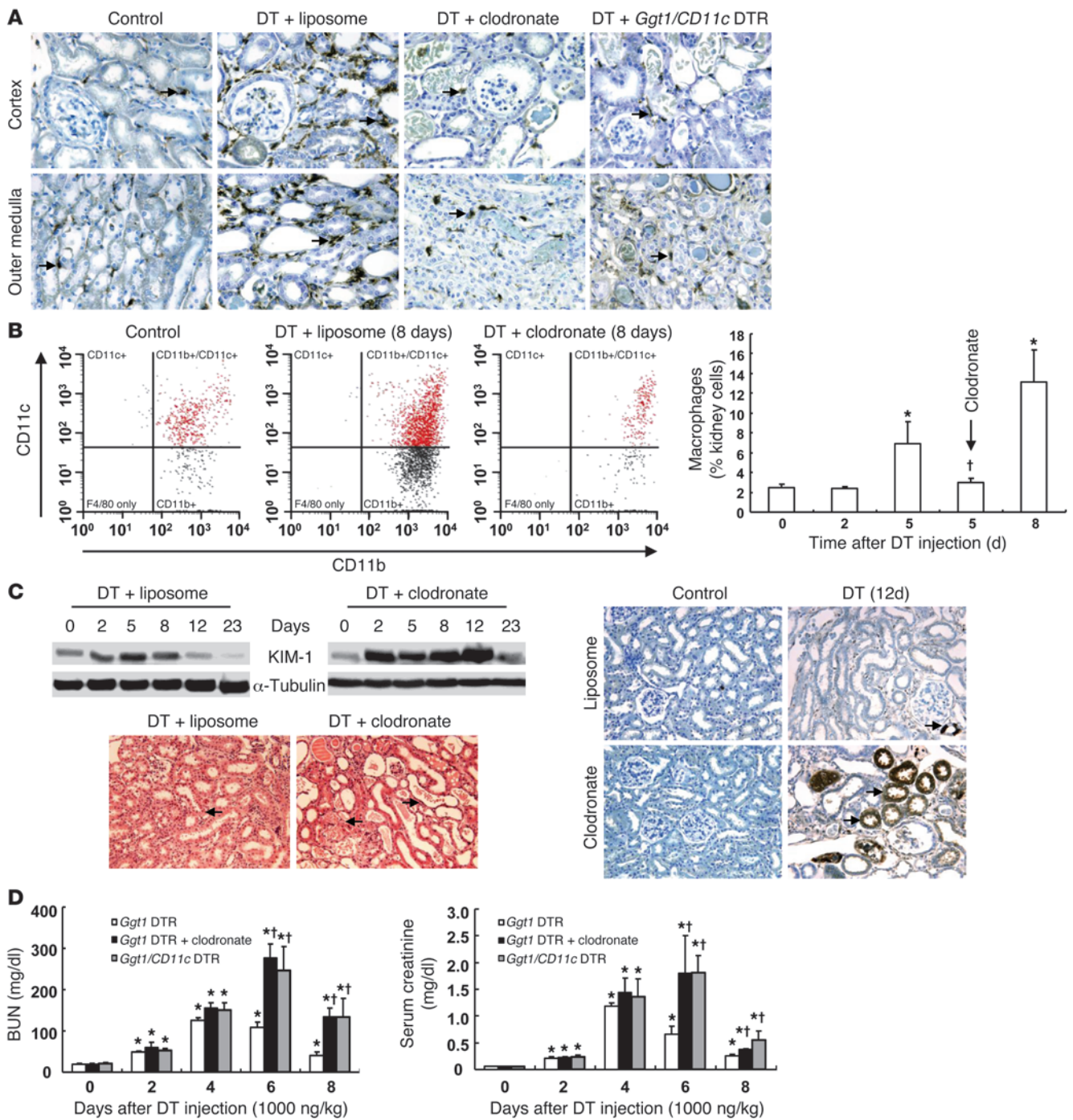
Figure 3
Macrophages/dendritic cells were involved in recovery from DT-mediated AKI in *Ggt1* DTR mice. (**A**) DT injection for 8 days led to increased F4/80hi cells (arrows) in the kidney, which were markedly reduced by clodronate treatment or in *Ggt1/CD11c* DTR double-transgenic mice. Original magnification, ×250. (**B**) Flow cytometric analysis determined that F4/80hi cells were markedly increased in the kidney 5 and 8 days after DT injection, and macrophage/dendritic cell depletion led to reduced kidney F4/80hi cells (*$P < 0.01$ vs. baseline; †$P < 0.01$ vs. corresponding liposome group; $n = 6$). (**C**) Macrophage/dendritic cell depletion did not increase renal KIM-1 expression in control mice, but led to increased and prolonged KIM-1 expression in DT-treated mice. Original magnification, ×160. 12 days after DT injection, histologic kidney damage (arrows) was still evident in *Ggt1* DTR mice with macrophage/dendritic cell depletion. Original magnification, ×100. (**D**) Levels of serum BUN and creatinine remained higher during recovery from DT-mediated AKI in mice with macrophage/dendritic cell depletion (*$P < 0.01$ vs. baseline; †$P < 0.01$ vs. corresponding liposome group; $n = 5$ per group).

Table 1
Phenotype of kidney F4/80^{lo} and F4/80^{hi} macrophages in DT-mediated AKI (5 days)

	CD11b	CD11c	Ly6C	Gr-1	CD62L	CX3CR1	CD86	MHCII (IA)
F4/80^{lo}	High	–	+	+	+	–	–	–
F4/80^{hi}	Low	+	–	–	–	+	+	+

cells in control kidney, liver, and spleen (Supplemental Figure 5) and blunted increases in renal F4/80^{hi} cells after DT administration (Figure 3, A and B). Macrophage/dendritic cell depletion induced a striking increase in histologic damage as well as increased TUNEL staining and expression of the tubule injury marker KIM-1 (Figure 2D and Figure 3C). Serum BUN and creatinine confirmed increased kidney dysfunction and delayed recovery (Figure 3D). Clodronate depletion of macrophages/dendritic cells during the recovery phase from renal I/R injury also delayed recovery (Supplemental Figure 2), consistent with previous reports (24). Depletion of renal macrophages/dendritic cells expressing CD11c by administration of DT to transgenic mice expressing the DTR in both proximal tubule and in CD11c$^+$ cells (referred to herein as *Ggt1/CD11c* DTR double-transgenic mice) produced similar delays in structural and functional recovery (Figure 3, A and D, and Supplemental Figure 6).

Depletion of F4/80^{hi} cells markedly decreased renal epithelial regeneration after DT treatment, as indicated by a delayed and attenuated peak of Ki67 expression (Figure 2E). Previous studies have indicated roles for EGF-like growth factors (16), CSF-1 (28), and MSP-1 (10) in recovery from acute renal epithelial injury. In kidneys of DT-treated mice, increased receptor phosphorylation for the EGFR, the CSF-1 receptor (c-fms), and the MSP-1 receptor (Ron-β) was markedly blunted with clodronate treatment (Figure 4A). With renal macrophage/dendritic cell depletion, there was also a persistent increase in renal neutrophil infiltration in response to DT administration (Figure 4B).

Although a dose of 100 ng/kg DT did not induce death in transgenic mice administered liposomes alone, clodronate-induced macrophage/dendritic cell depletion led to 60% mortality by 15 days (Figure 4C). The increased mortality was not different when mice were administered clodronate 2 days prior to or 1 day after DT administration. A similar increase in mortality was seen with selective depletion of CD11c$^+$ cells by DT administration to *Ggt1/CD11c* DTR double-transgenic mice (Figure 4C). The clodronate-treated mice that survived exhibited increased tubulointerstitial fibrosis and persistent albuminuria (Figure 4, D and E).

We next quantified renal expression of cytokines and other proteins associated with M1 or M2 macrophage phenotypes using quantitative real-time RT-PCR (qRT-PCR). In response to I/R-induced renal injury, there were increases in the kidney of M1 markers (*iNOS* and *Ccl3*) that were higher at 18 hours than 72 hours after injury, whereas M2 markers (*Arg1*, encoding arginase; and *Igf2r*, encoding mannose receptor [MR]) were much higher at 72 hours than 18 hours after injury (Figure 5A). Although DT administration led to early induction of *Il23a*, there were similar increases in clodronate-treated mice (Figure 5B), indicative of a nonmonocyte source. There were not statistically significant increases in mRNA of other M1 markers (*iNOS* and *Ccl3*) in response to DT, nor were there any differences in expression between liposome- and clodronate-

treated mice. In contrast, mRNA expression of the M2 markers *Arg1*, *Igf2r*, and *Il4ra* (encoding IL-4 receptor α [IL-4Rα]; also known as CD124) all increased significantly after DT treatment in the liposome-treated mice, while there were minimal increases, if any, in the clodronate-treated mice. Expression of the M2 marker *Tgfb* increased significantly in response to DT, and clodronate markedly delayed this increase and induced persistently elevated *Tgfb* expression (Figure 5C). A similar increase in M2 markers was seen in cells isolated from kidneys by CD11b beads, with significant blunting in clodronate-treated and in *Ggt1/CD11c* DTR double-transgenic mice (Figure 5D). Similar results were also observed with isolation by CD11c beads (Supplemental Figure 7A). Immunoblotting revealed increased renal expression of IL-4Rα, MR, and arginase proteins in response to DT, and these increases were also blunted in clodronate-treated mice (Figure 5E). Immunoblotting also confirmed increased arignase protein expression in isolated kidney reparative macrophages/dendritic cells after DT injection (Supplemental Figure 7B).

To investigate the source of the increased renal macrophages/dendritic cells mediating the epithelial cell recovery after DT administration or I/R injury, we isolated splenic monocytes, labeled them ex vivo with the monocyte-specific dye PKH26, and injected 2×10^6 cells into control mice, mice undergoing bilateral I/R injury (4 hours before surgery), or mice with DT-mediated injury. Animals were sacrificed at the indicated times, and the number of labeled cells in the kidney was quantified. As shown in Figure 6A, there was a 15-fold increase in the number of labeled monocytic cells detected in the kidney within 1 day after I/R. In contrast, the number of infiltrating monocytes after DT administration did not increase above that seen in control mice. In vitro polarization of splenic monocytes to either an M1 or M2 phenotype prior to injection into DT-treated mice did not increase the number of labeled cells detected in the kidney (data not shown). Prior splenectomy did not alter the pattern of recovery or significantly alter the number of F4/80^{hi} cells or neutrophils in the kidney after DT administration (Supplemental Figure 8). We also isolated bone marrow cells enriched for the marker Ly6C, labeled them ex vivo with PKH26, and injected 5×10^6 cells into control mice, mice undergoing bilateral I/R injury (4 hours before surgery), or mice with DT-mediated injury. As shown in Figure 6B, there was a marked increase in the number of labeled bone marrow Ly6C$^+$ cells in the kidney after I/R (390% increase 3 days after I/R) compared with DT administration (90% increase 3 days after DT administration; $P < 0.001$, DT vs. I/R).

We used flow cytometry to determine whether there was in situ proliferation of renal macrophages and dendritic cells during recovery from AKI. After DT administration, there was a significant increase in the percentage of F4/80^{hi} cells isolated from kidneys that colabeled with the proliferation marker Ki67 (control, $0.41\% \pm 0.09\%$ Ki67$^+$ of total kidney cells; day 5 after DT, $4.16\% \pm 1.25\%$; $P < 0.01$; $n = 6$; Figure 6C). Furthermore, there was a significant increase in the percentage of kidney F4/80^{hi} cells colabeling with another proliferation marker, BrdU (control, $0.09\% \pm 0.02\%$ BrdU$^+$ of total kidney cells; day 5 after DT, $1.01\% \pm 0.06\%$; $P < 0.01$; $n = 3$; Figure 6D). Similarly, after I/R injury, Ki67$^+$F4/80^{hi} cells in the kidney began to increase by 1 day after injury (day 0, $0.19\% \pm 0.03\%$ Ki67$^+$F4/80^{hi} of total kidney cells; day 3 after I/R, $2.50\% \pm 0.66\%$; $P < 0.01$; $n = 4$; Figure 6E).
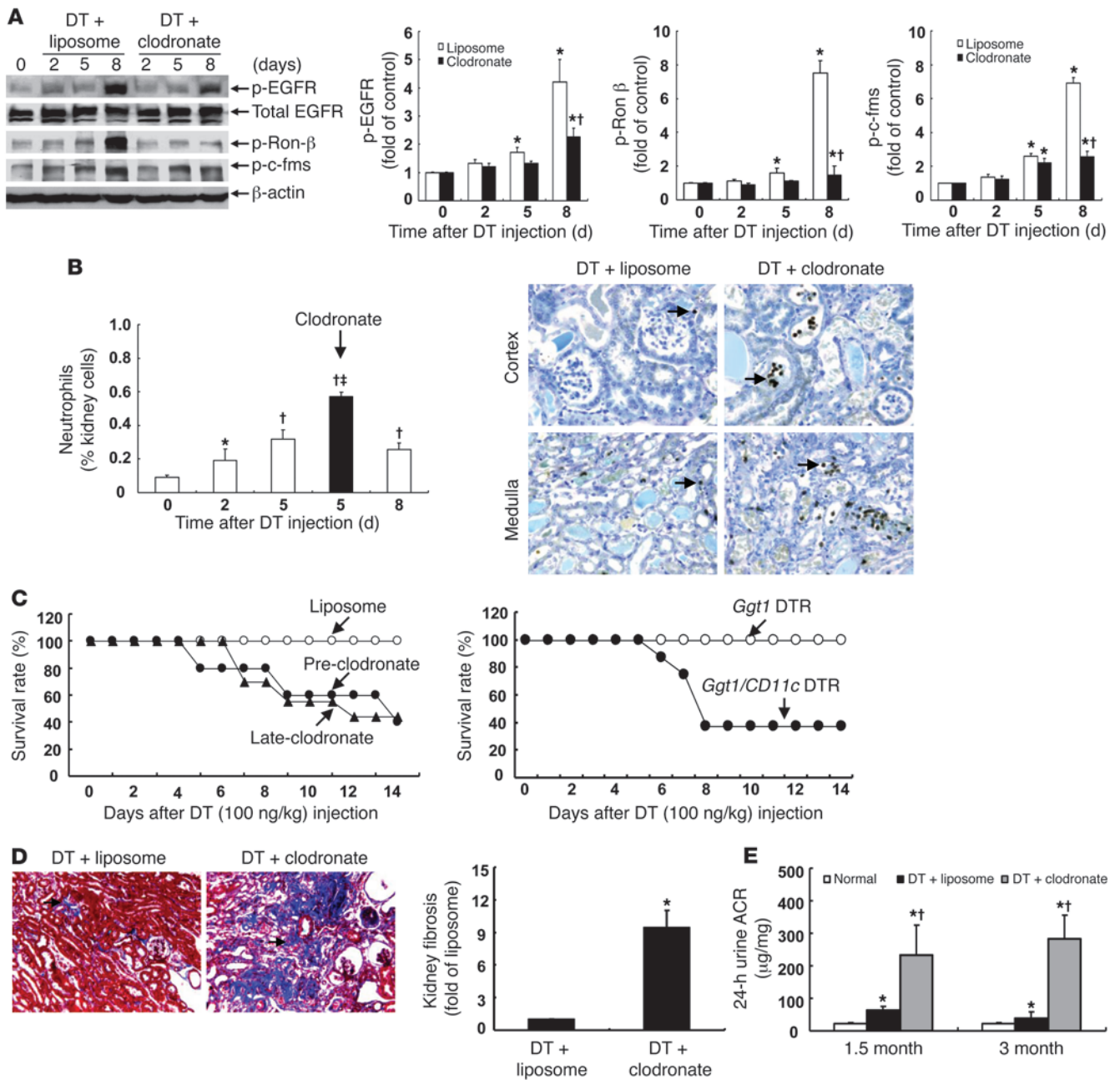
Figure 4
Macrophages/dendritic cells played key roles in recovery from DT-mediated AKI in *Ggt1* DTR mice. (**A**) Macrophage/dendritic cell depletion inhibited activation of EGFR, Ron-β, and c-fms pathways (*$P < 0.01$ vs. baseline; †$P < 0.01$ vs. corresponding liposome group; $n = 3$ per group). (**B**) Flow cytometric analysis determined that Gr-1+ neutrophils increased after DT injection and that macrophage/dendritic depletion significantly increased the neutrophil infiltration (*$P < 0.05$, †$P < 0.01$ vs. baseline; ‡$P < 0.05$ vs. corresponding liposome group; $n = 4$–6). Representative photomicrographs indicate increased neutrophil infiltration in kidneys from clodronate-treated *Ggt1* DTR mice 5 days after DT injection (arrows). Original magnification, ×250. (**C**) Pharmacologic (clodronate) or genetic (*Ggt1/CD11c* DTR) depletion of macrophages/dendritic cells led to increased mortality in DT-mediated AKI mice (pre-clodronate [administered 2 days prior to DT] and late-clodronate [administered 1 day after DT], $P < 0.01$ vs. liposome, $n = 8$–10; genetic depletion, $P < 0.001$ vs. *Ggt1* DTR, $n = 8$ per group). (**D**) 3 months after DT injection, survivors of clodronate treatment had markedly higher kidney interstitial fibrosis (arrows), indicated by Masson Trichrome staining (*$P < 0.01$ vs. liposome group; $n = 4$ per group). Original magnification, ×100. (**E**) Survivors of clodronate treatment had persistent albuminuria (*$P < 0.01$ vs. control; †$P < 0.01$ vs. corresponding liposome group; $n = 6$ per group). ACR, albumin/creatinine ratio.
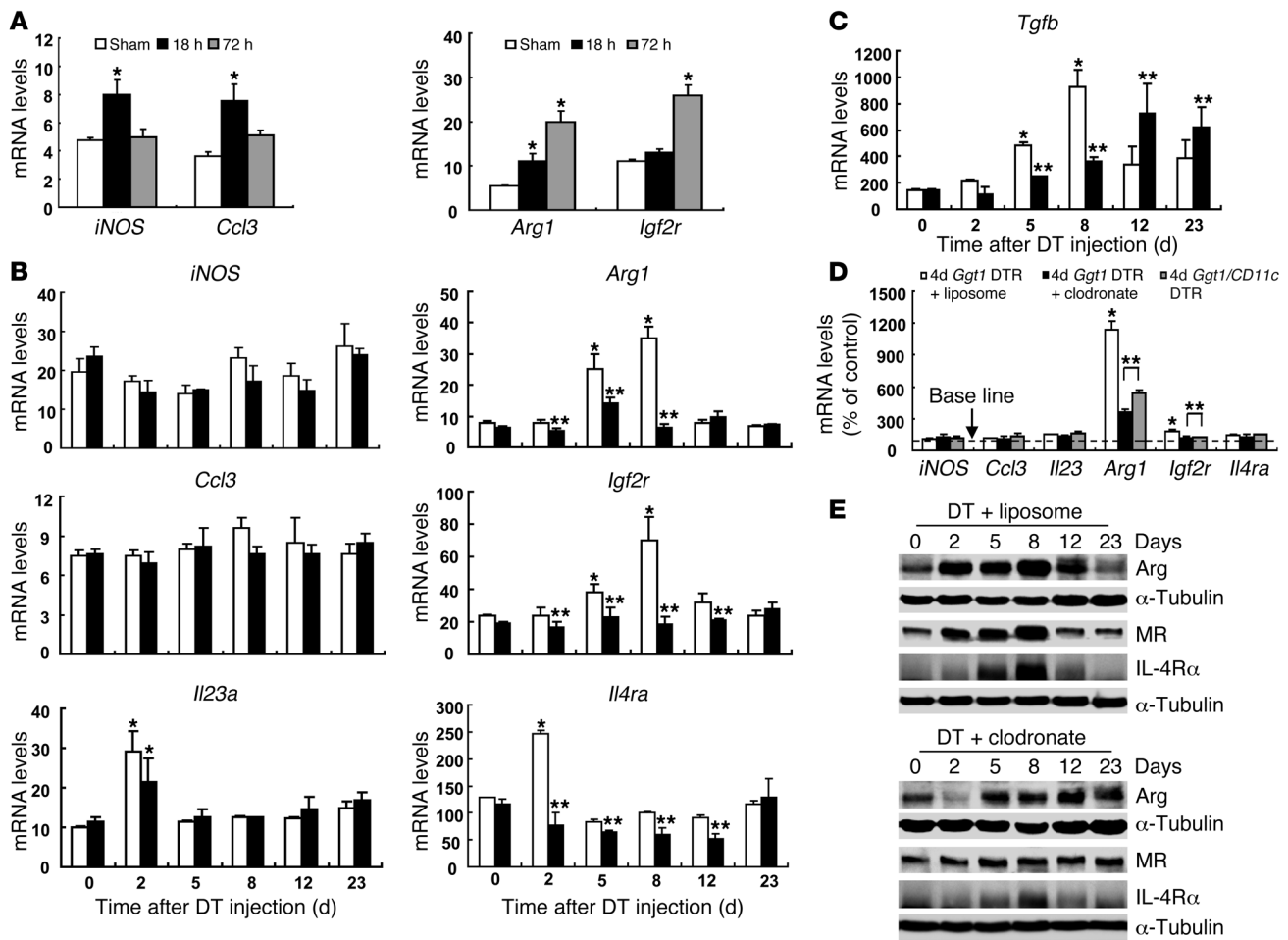
Figure 5

Markers of M1 and M2 macrophages in kidney of AKI. (**A**) M1 markers (*iNOS* and *Ccl3*) were increased by 18 hours after initiation of I/R injury (*P < 0.05 vs. sham; n = 4), while M2 markers were elevated after 72 hours (*P < 0.01 vs. sham; n = 4). (**B**) In *Ggt1* DTR mice, DT led to early increases in mRNA levels of the M2 markers *Arg1*, *Igf2r*, and *Il4ra*, which were markedly reduced by macrophage/dendritic cell depletion. Expression of M1 markers (*iNOS*, *Ccl3*, and *Il23a*) was not affected by clodronate treatment. White bars, liposome vehicle; black bars, clodronate (*P < 0.01 vs. control; **P < 0.01 vs. corresponding liposome group; n = 3–5). (**C**) Macrophage/dendritic cell depletion led to attenuated but persistent increases in *Tgfb* mRNA levels (*P < 0.01 vs. control; **P < 0.01 vs. corresponding liposome group; n = 3–5). (**D**) Pharmacologic (clodronate) or genetic (*Ggt1/CD11c* DTR) depletion of macrophages/dendritic cells had no effect on the mRNA levels of *iNOS*, *Ccl3*, and *Il23a*, but significantly reduced mRNA levels of *Arg1* and *Igf2r*, in isolated macrophages/dendritic cells from kidneys after DT administration for 4 days (*P < 0.01 vs. control; **P < 0.01 vs. corresponding liposome group; n = 3–5). (**E**) Western analysis indicated increased levels of arginase (Arg), MR, and IL-4Rα in response to DT administration, which were reduced by macrophage/dendritic cell depletion.

In response to DT injection, renal *Csf1* mRNA levels were increased as early as 2 days after DT injection, and immunostaining determined that increased CSF-1 expression was primarily localized to epithelial cells (Supplemental Figure 9A). GW2580, an inhibitor of c-fms (29), inhibited c-fms phosphorylation in response to DT-induced injury and exacerbated increases in BUN and creatinine, with development of increased interstitial fibrosis (Figure 7A and Supplemental Figure 9B). GW2580 not only decreased macrophage/dendritic cell proliferation (vehicle, 7.83% ± 2.31% of total kidney cells on day 5; GW2580, 1.56% ± 0.19%; P < 0.05; n = 4; Figure 7B), it also markedly inhibited expression of M2 markers and increased expression of M1 markers in renal macrophages/dendritic cells isolated from the DT model on day 5 (Figure 7C). Similarly, in response to I/R injury, GW2580 not only inhibited the progressive decreases in BUN normally seen from day 1 to

day 3 (Figure 7D), it also markedly decreased the number of renal macrophages/dendritic cells (vehicle, 3.03% ± 0.57% of total kidney cells; GW2580, 1.44% ± 0.18%; P < 0.05; n = 4) and significantly reduced the in situ renal proliferation of these cells on day 3 (vehicle, 2.50% ± 0.66% of total kidney cells; GW2580, 0.91% ± 0.23%; P < 0.05; n = 4; Figure 7D).

To confirm that inhibition of CSF-1 signaling underlay the effects seen with GW2580, we used *Csf1*−/− mice. In the DT model of AKI, BUN increased to significantly higher levels in *Csf1*−/− mice than in WT controls. There was persistent renal injury and increased tubulointerstitial fibrosis in *Csf1*−/− mice 12 days after DT injection (Figure 8A). There were also significantly decreased total (WT, 10.40% ± 2.41% of total kidney cells; *Csf1*−/−, 1.49% ± 0.11%; P < 0.001; n = 4) and proliferating (WT, 7.63% ± 1.59% of total kidney cells; *Csf1*−/−, 0.78% ± 0.11%; P < 0.001; n = 4) renal macrophages/
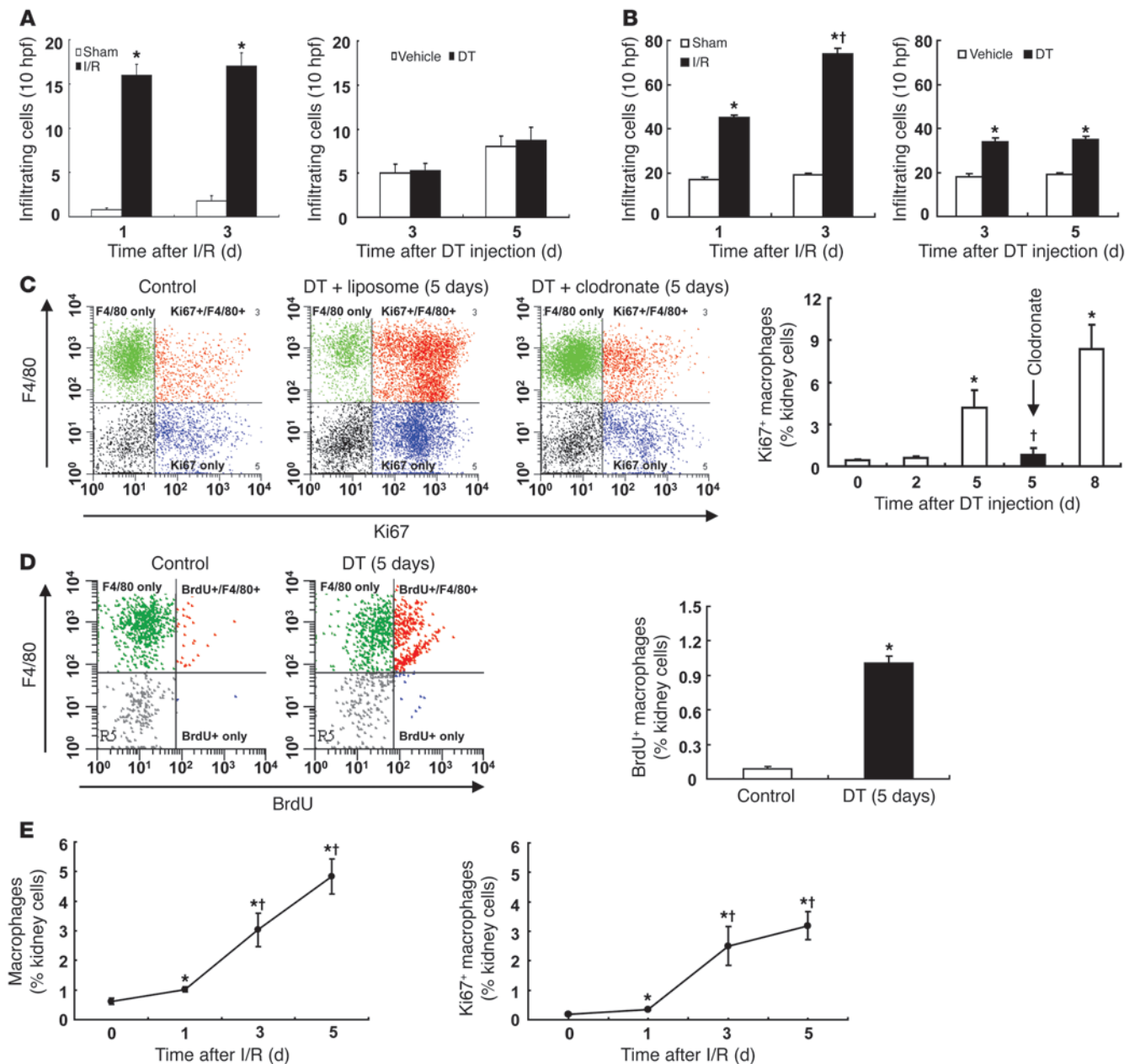
Figure 6

Renal macrophages/dendritic cells proliferated after DT administration. (**A**) I/R caused rapid kidney infiltration of PKH26-labeled splenic monocytes versus sham animals (*P < 0.001 vs. sham; n = 3 per group), while kidney infiltration of PKH26-labeled splenic monocytes was comparable between vehicle- and DT-treated *Ggt1* DTR mice at 3 and 5 days (2 × 10⁶ cells/mouse i.v.; n = 5 per group). (**B**) With I/R injury, there was rapid and significant kidney infiltration of PKH26-labeled Ly6C⁺-enriched bone marrow cells compared with sham animals (*P < 0.01 vs. sham); 3 days after injury, there was a 390% increase. In DT-treated mice, PKH26-labeled Ly6C⁺-enriched bone marrow cells increased 90% at 3 days compared with vehicle-treated animals (*P < 0.01 vs. vehicle), significantly less than at the same time point after I/R injury (†P < 0.001, I/R vs. DT at 3 days), with no further increase at 5 days (5 × 10⁶ cells/mouse i.v.). (**C**) DT administration (5 days) markedly increased reparative macrophage/dendritic cell proliferation (Ki67⁺F4/80ʰⁱ cells), which was attenuated by macrophage/dendritic cell depletion (*P < 0.01 vs. baseline; †P < 0.01 vs. corresponding liposome group; n = 6). (**D**) 5 days after DT administration, macrophages/dendritic cells that were BrdU⁺F4/80ʰⁱ markedly increased (*P < 0.01 vs. control; n = 3). (**E**) In response to I/R injury, both total macrophages and proliferating macrophages markedly increased as early as 1 day after injury and peaked at 3 days (*P < 0.05 vs. baseline; †P < 0.01 vs. 1 day after injury; n = 4).

dendritic cells on day 5, and there were significant increases in M1 markers and decreases in M2 markers on macrophages/dendritic cells isolated from *Csf1*⁻/⁻ mice (Figure 8, B and C). Similarly, with I/R injury, functional renal recovery was delayed (Supple-

mental Figure 10), and the number of total (control, 0.76% ± 0.21% of total kidney cells; WT I/R, 4.49% ± 1.35%; *Csf1*⁻/⁻ I/R, 0.99% ± 0.14%; P < 0.05, *Csf1*⁻/⁻ vs. WT; n = 4) and proliferating (control, 0.26% ± 0.07% of total kidney cells; WT I/R, 3.62% ± 1.30%;
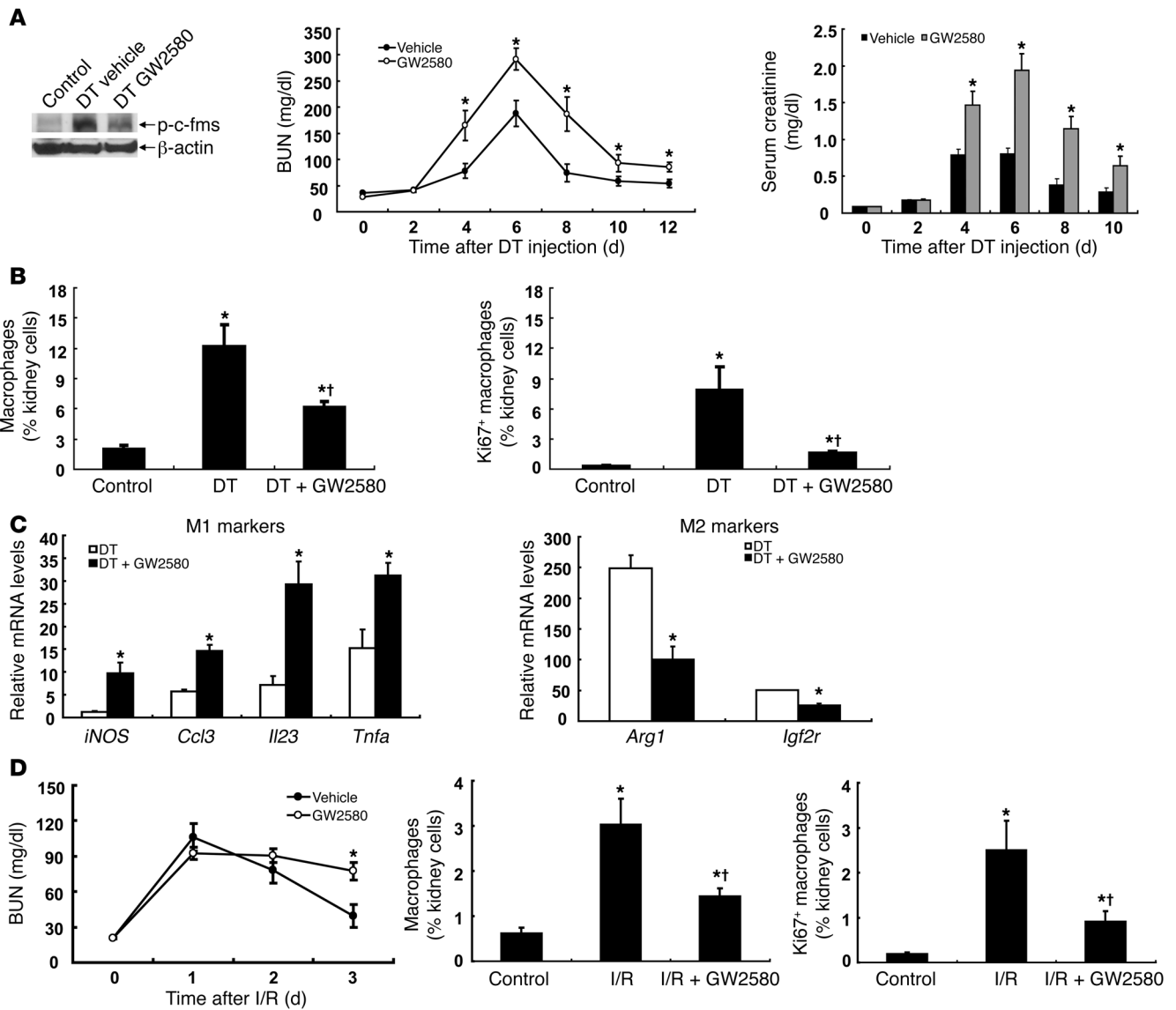
Figure 7

Activation of c-fms is necessary for macrophage/dendritic cell proliferation and polarization to an M2 phenotype during recovery from AKI. (**A**) GW2580 markedly inhibited the activity of c-fms. GW2580 augmented DT-mediated AKI, as indicated by increased serum BUN and creatinine (*$P < 0.05$ vs. vehicle; $n = 6$ per group). (**B**) Flow cytometry demonstrated that GW2580 inhibited DT-mediated increases in resident macrophage/ dendritic cell proliferation and increases in total F4/80^{hi} cells 5 days after DT injection (*$P < 0.001$ vs. baseline; †$P < 0.05$ vs. vehicle group; $n = 4$). (**C**) GW2580 led to increases in expression of M1 markers and decreases in expression of M2 markers in renal macrophages/dendritic cells 5 days after DT injection (*$P < 0.05$ vs. corresponding vehicle group; $n = 4$ per group). (**D**) GW2580 delayed functional recovery and inhibited the increases in total and proliferating macrophages/dendritic cells in response to I/R injury on day 3 (*$P < 0.001$ vs. baseline; †$P < 0.05$ vs. vehicle; $n = 4$).

$Csf1^{-/-}$ I/R, $0.82\% \pm 0.11\%$; $P < 0.05$, $Csf1^{-/-}$ vs. WT; $n = 4$) renal macrophages/dendritic cells was significantly decreased at day 3 (Figure 8D). In addition, there was a persistence of macrophages/ dendritic cells expressing M1 markers and a decrease in expression of M2 markers (Figure 8E).

Discussion

Using 2 distinct models of AKI, caused either by I/R or by administration of DT to transgenic mice selectively expressing the human DTR in proximal tubule, we found an important role for in situ proliferation and differentiation of renal macrophages/dendrit-

ic cells in renal epithelial repair. Both the proliferation and the polarization of the renal macrophage and dendritic cells during the reparative phase were crucially dependent on CSF-1 signaling.

After I/R injury, renal endothelial cells upregulate the expression of CX3CL1 (fractalkine), a ligand for the CX3CR1 receptor that is expressed on circulating monocytes and macrophages (8). This interaction mediates the macrophage infiltration that is seen within 1 hour of reperfusion. Increased interstitial macrophages can be detected in the cortex and outer stripe of the outer medulla early in the course of rodent models of ischemic and toxic injury (29–33). As previously reported (24, 30, 31), and confirmed in the current stud-
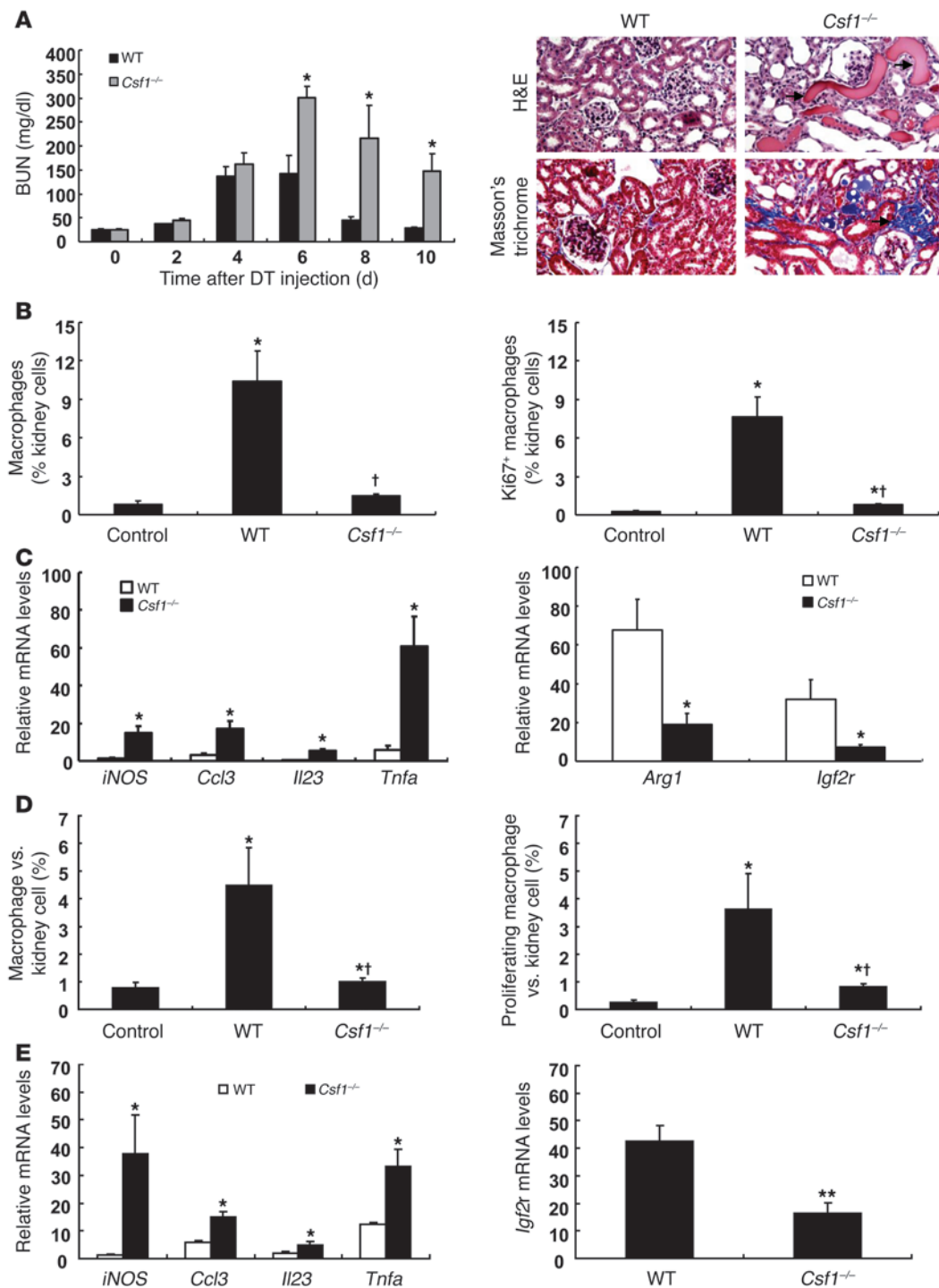
Figure 8
CSF-1 is essential for recovery from AKI through promoting macrophage/dendritic cell proliferation and polarization to an M2 phenotype. (**A**) CSF-1 deficiency augmented DT-mediated AKI, as indicated by increased BUN (*$P < 0.05$ vs. WT; $n = 6$ per group) and by delayed histologic recovery (arrows) 12 days after DT administration. Original magnification, ×160. (**B** and **C**) CSF-1 deficiency markedly inhibited DT-mediated increases in total and proliferating resident macrophages/dendritic cells (*$P < 0.001$ vs. control; †$P < 0.01$ vs. WT; $n = 4$; **B**), decreased expression of M2 markers, and increased expression of M1 markers in isolated renal macrophages/dendritic cells 5 days after DT injection (*$P < 0.05$ vs. WT; $n = 4$; **C**). (**D**) CSF-1 deficiency attenuated the increases in both total and proliferating renal macrophages/dendritic cells in response to I/R injury on day 3 (*$P < 0.05$ vs. control; †$P < 0.05$ vs. WT; $n = 4$). (**E**) CSF-1 deficiency increased levels of M1 markers and decreased levels of M2 markers in isolated macrophages/dendritic cells 3 days after I/R injury (*$P < 0.05$, **$P < 0.01$ vs. WT; $n = 4$–6).

ies, these macrophages infiltrating early after I/R injury had a distinct phenotype consistent with inflammatory or M1 macrophages. Macrophages are a source of proinflammatory cytokines, including IL-1, IL-6, and TNF-α, that are detected after AKI (30, 32, 33).

Macrophage depletion prior to I/R injury (7, 8, 34) or inhibition of macrophage influx into the kidney (35) will decrease the degree of renal injury induced by I/R. Similar protection by prior macrophage depletion has also been reported in models of acute inflammatory injury of other organs (36, 37). In contrast, recent studies have indicated that when macrophages/dendritic cells are depleted later in the recovery phase after AKI, there are delayed rates of structural and functional recovery (24, 38, 39). In the current studies, we confirmed that there is an important role for reparative macrophages/dendritic cells in recovery from I/R injury and also found that depletion of reparative macrophages/dendritic cells either prior to or after initiation of a model of predominantly apoptotic epithelial injury had similar effects to markedly inhibit recovery.

It is now well recognized that monocyte-derived cells serve numerous functions and manifest a variety of phenotypes. This variation was originally designated as polarization of macrophages to an M1 or M2 (noninflammatory) phenotype (40). In the current studies, the predominant monocyte phenotypic markers seen in the kidney after DT administration or during the recovery phase from I/R injury were those associated with an M2 phenotype. The increased injury and profound delay in recovery in response to macrophage/dendritic cell depletion either prior to or after administration of DT is indicative of an important role for the M2 phenotype in repair and regeneration after acute epithelial injury.

While the classic paradigms argue that infiltrating macrophages convert from an M1 to an M2 phenotype or that M1 macrophages derive from circulating monocytes that express Ly6C and M2 macrophages from circulating monocytes deficient in Ly6C (24, 41–43), new evidence is emerging for an important additional role for in situ proliferation of tissue macrophages in mediation of Th2-mediated responses (44). Our studies indicate that both after DT administration and in I/R injury, proliferation of renal macrophages/dendritic cells serves as an important source of cells mediating the tubule repair. Our results indicate that in the DT model, the proliferating cells were predominantly intrinsic renal macrophages and dendritic cells. We did not detect any increase in labeled spleen-derived monocytes after DT administration and found only a relatively small increase in Ly6C-enriched bone marrow–derived monocytes 3 days after DT administration, with no further increase at 5 days (Figure 6B). Since we did detect significant increases in renal accumulation of either splenocytes or bone marrow–derived monocytes after I/R, it is possible that in I/R, infiltrating cells may also proliferate and convert from an M1 to an M2 phenotype. Of note, in preliminary studies, fractalkine expression did not markedly increase in the kidneys after DT-induced injury.

CSF-1 is an important mediator of tissue macrophage proliferation and differentiation (45), and there was activation of c-fms in response to DT administration (Figure 4A). Expression of CSF-1 in the kidney increases in response to I/R injury (26), and *Csf1* mRNA levels markedly increased as early as 2 days after DT injection (Supplemental Figure 9A). Although CSF-1 has been shown to stimulate renal epithelial cell proliferation directly after I/R injury to the kidney (28), in the DT models of tubule injury, the partial inhibition of c-fms phosphorylation in the clodronate-treated mice was also suggestive of renal macrophage/dendritic cell activation.

Furthermore, in mice with genetic deletion of *Csf1*, as well as in WT mice treated with a pharmacologic inhibitor of c-fms, there were marked decreases in the proliferation and polarization to an M2 phenotype of renal macrophages and dendritic cells during the recovery phase from injury in both the DT and the I/R models.

IL-4 and IL-13 are known to induce macrophage polarization to an M2 phenotype via JAK3/STAT6 activation, and their receptors share a common subunit, IL-4Rα (46). However, previous studies by Lee et al. suggested that injured proximal tubule cells may induce M2 polarization of macrophages through an IL-4– and IL-13–independent mechanism (24), and recent studies have indicated that CSF-1 can mediate proliferation and polarization of macrophages and dendritic cells in uterine tissues (38). Given that injured proximal tubule cells produce CSF-1 (26), our results therefore indicate an important role for renal CSF-1 in the polarization to an M2-like phenotype of renal macrophages and dendritic cells that are playing an indispensable role in mediating renal epithelial cell regeneration.

Tissue macrophages and dendritic cells have been shown to play an essential role in tissue repair in other organs (21–23). Reparative macrophages and dendritic cells can release growth factors that can accelerate wound and tissue repair (39, 41, 47). Release of growth-promoting substances would be consistent with the evidence of delayed onset and reduced intensity of epithelial proliferation seen with macrophage/dendritic cell depletion. In addition, arginase allows macrophages to convert arginine to ornithine, a precursor of collagens and polyamines, which are important for cell growth and extracellular matrix production.

Reparative macrophages are also phagocytes. There is evidence that when apoptotic cells are not phagocytosed, they may eventually rupture and release their cellular contents, a process known as *secondary necrosis*, and these cellular contents may activate viable epithelial cells and infiltrating cells through Fc receptors and TLRs and induce inflammatory cytokines (42). In this regard, in the current studies, macrophage/dendritic cell depletion prior to induction of renal epithelial apoptosis resulted in markedly increased and prolonged neutrophil infiltration (Figure 4B). Furthermore, macrophages that engulf apoptotic cells produce TGF-β, which can inhibit inflammatory responses (43), while engulfment of necrotic cells induces macrophages to produce inflammatory cytokines (42, 48). Of note, *Tgfb* expression increased significantly in the kidney after DT administration, but with clodronate treatment, the initial increase in *Tgfb* was blunted and delayed, and expression persisted for up to 23 days after onset of injury (Figure 5C), consistent with the increased tubulointerstitial fibrosis occurring as a result of macrophage/dendritic cell depletion. This finding suggests that the initial increases in *Tgfb* may be derived from macrophages/dendritic cells, whereas the secondary increases seen in the clodronate-treated mice may be derived from intrinsic renal sources (i.e., epithelial cells and/or fibroblasts).

Although the cells involved in mediating recovery from the DT-induced tubule injury are of monocyte origin, whether these cells should be classified as *tissue macrophages* or *dendritic cells* is an area of controversy in the field (49). After DT-mediated injury, there is an increase in F4/80^{hi} cells, previously considered a marker of macrophage/monocytes, but not dendritic cells; however, this distinction has been questioned since tissue-specific dendritic cells also express this marker (50). Similarly, dendritic cells may also express M2 macrophage markers, such as arginase and MR. Our studies using *Ggt1/CD11c* DTR double-transgenic mice indicated that

CD11c^{+} cells are crucial for the recovery process. Although CD11c was previously considered to be specific for dendritic cells, it is now recognized that it is also expressed on tissue macrophages, and the macrophage marker CD11b is also expressed on tissue dendritic cells (20). Flow cytometric analysis indicated that the increased CD11b^{hi}F4/80^{hi}CD11c^{+} cells expressed cell surface markers consistent with dendritic cells, whereas CD11b^{hi}F4/80^{hi}CD11c^{−} cells had a phenotype consistent with tissue macrophages (Table 1 and ref. 27), which suggests that both dendritic cells and tissue macrophages proliferate and increase in number in response to DT-mediated or I/R injury. It is possible that these subsets of cells may have overlapping actions or serve separate functions (51), such as efferocytosis by tissue macrophages and tissue repair by dendritic cells, but further studies will be required for complete cataloging and determination of function of these cellular subsets.

In summary, our results demonstrated an important role for renal macrophages/dendritic cells to mediate regeneration after AKI. These F4/80^{hi} cells expressed markers consistent with alternatively activated macrophages. We conclude that activation of c-fms is necessary for in situ renal macrophage/dendritic cell proliferation and for polarization to an M2 phenotype. The importance of proliferation of intrinsic tissue macrophages and dendritic cells as a source of these cells was clearly shown after DT-induced proximal tubule cell apoptosis, in which infiltrating monocytes were not detected. Such in situ expansion and polarization of resident renal macrophages/dendritic cells in AKI represents an important but previously unrecognized mechanism by which the kidney can effect its own repair.

Methods

Generation of Ggt1 DTR transgenic mice. The human HB-EGF coding sequence was amplified using gene-specific (Genbank accession no. NM_001945) primers with custom restriction sites by PCR, using full-length human HB-EGF cDNA as template. The antisense primer sequence also contained the HA-tag sequence and thus resulted in C-terminal incorporation of an HA-tag in the 3′ end of the amplified sequence. A DNA fragment that contained a polyadenylation (PolyA) signal of the human growth hormone gene was further combined at the 3′ end of the human HB-EGF–HA tag sequence using a custom-created restriction site. The resultant HB-EGF–HA–PolyA DNA was then ligated to the 3′ end of the Ggt1 promoter (2.3 kb; gift of M. Lieberman, Baylor College of Medicine, Houston, Texas, USA), which has previously been used successfully to target genes of interest primarily to the renal proximal tubule (52, 53). The resultant transgene DNA was injected into fertilized eggs of B6D2 mice at the Transgenic/ES Cell Shared Resource Core, Vanderbilt University Medical Center. The integration of the transgene was identified by PCR and confirmed by Southern blot analysis. We identified 12 founders expressing the transgene and used 3 founders for subsequent characterization.

Animal studies. Adult male heterozygous transgenic mice were used for the experiments. All mice were genotyped with PCR before use.

CD11c DTR transgenic mice (B6.FVB; Itgax-DTR/EGFP) obtained from the Jackson Laboratory were crossed with Ggt1 DTR transgenic mice to generate Ggt1/CD11c DTR double-transgenic mice. The primers 5′-GCCACACCAAACAAGGAGGAGCAC-3′ (forward) and 5′-GCGTA-ATCTGSSACATCGTATGGG-3′ (reverse) generated a 370-bp product of HA-tag in Ggt1 DTR mice, while primers oIMR0872 and oIMR1416 generated a 173-bp product of GFP in CD11c DTR mice.

Heterozygous B6;C3Fe a/a-Csf1[op/J] mice (Csf1^{−/+}, stock no. 000231; Jackson Laboratory) were crossed with Ggt1 DTR transgenic mice to generate Csf1^{−/−}Ggt1 DTR mice, which were further crossed with original Csf1^{−/+} mice

to generate Csf1^{+/+}Ggt1 DTR and Csf1^{−/−}Ggt1 DTR mice, respectively. For experiments, Csf1^{+/+}Ggt1 DTR mice and Csf1^{−/−}Ggt1 DTR mice from the same litters were used.

AKI was initiated by i.p. injection of DT (Sigma-Aldrich). Although many mammals are sensitive to DT, rodents are 10^3–10^6 times more resistant, since DT does not bind to their HB-EGF (54). Therefore, selective expression of human HB-EGF in cells of interest allows induction of targeted injury. Monocyte/macrophage depletion was induced by i.p. administration of clodronate (Encapsula NanoSciences) at a dose of 40 mg/kg initially, then 20 mg/kg every 3 days thereafter throughout the experiment. As controls, mice were given the liposome carrier alone. GW2580 (LC laboratories), an inhibitor of c-Fms, was given at a dose of 70 mg/kg (gastric gavage, twice per day) throughout the experiment. BrdU was administered at a dose of 20 mg/kg/d through subcutaneous osmotic minipumps (model 2001; Alzet) plus 1 mg i.p. injection 2 hours before sacrifice. For urine collections, the animals were first acclimated individually in metabolic cages, and then 24-hour urine was collected. Contralateral uninephrectomy followed by unilateral I/R with renal artery clamping for 30 minutes was performed as previously described (24). For experiments shown in Figure 5A and Figure 6, A and B, bilateral renal artery clamping for 35 minutes was used.

Immunofluorescence/immunohistochemistry staining and quantitative image analysis. The animals were anesthetized with Nembutal (70 mg/kg i.p.) and given heparin (1,000 U/kg i.p.) to minimize coagulation. One kidney was removed for Western analysis, flow cytometry, qRT-PCR, and histologic analysis, and the other was perfused with FPAS (3.7% formaldehyde, 10 mM sodium *m*-periodate, 40 mM phosphate buffer, and 1% acetic acid) through the aortic trunk cannulated by means of the left ventricle. The fixed kidney was dehydrated through a graded series of ethanols, embedded in paraffin, sectioned (4 μm), and mounted on glass slides. Immunostaining was carried out as in previous reports (55). For immunofluorescent staining, deparaffinized sections were blocked with 10% normal donkey serum for 1 hour and then incubated with primary antibodies overnight at 4°C. After washing with PBS, the sections were incubated with Rhodamine Red-X–conjugated donkey anti-goat IgG (Jackson ImmunoResearch Laboratories Inc.), washed with PBS, then incubated with fluorescein *L. tetragonolobus* agglutinin (green, FITC-labeled *L. tetragonolobus*, marker for proximal tubule epithelial cells; Vector Laboratories Inc.). Sections were viewed and imaged with a Nikon TE300 fluorescence microscope and spot-cam digital camera (Diagnostic Instruments). Based on the distinctive density and color of immunostaining in video images, the number, size, and position of stained cells were quantified using the BIOQUANT true-color windows system (R & M Biometrics) as previously described (56).

Apoptosis and proliferation. Cell proliferation was determined by Ki67 staining. The tissue sections were treated with Vector Antigen Unmasking solution for Ki67 antigen retrieval (Vector Laboratories). Apoptosis was detected by cleaved caspase-3 immunostaining and TUNEL assay as previously described (57).

Western blot analysis. Total kidney lysates were used for Western blot analysis as described previously (58).

Antibodies. Affinity-purified goat anti-DTR (human HB-EGF) and KIM-1 (a marker of renal tubular injury, MAB1817) were purchased from R&D Systems; rat anti-mouse F4/80 (MCA497R) and Ly6C (MCA2387T) were from AbD Serotec; affinity-purified rabbit anti-human IL-4Rα (NBP1-00884) and phospho–Ron-β were from Novus Biologicals; rabbit anti-MR (ab64693) was from Abcam; and antibodies against EGFR and p-EGFR, p–c-Fms, HA, arginase-1, Ki67, cleaved caspase-3, and cleaved caspase-9 were from Santa Cruz Biotechnology.

Flow cytometry. After perfusion of the kidneys with PBS, one kidney was removed, minced into fragments, and digested in RMPI 1640 containing 2 mg/ml collagenase type D and 100 μ/ml DNase I for 1 hour at 37°C,

with intermittent agitation. Kidney fragments were passed through a 70-μm mesh (Falcon; BD Biosciences), yielding single-cell suspensions. Cells were centrifuged (800 g, 10 minutes, 8°C), resuspended in FACS buffer, kept on ice, and counted. 10^7 cells were incubated in 2.5 μg/ml Fc blocking solution, centrifuged again (800 g, 10 minutes, 8°C), and resuspended with FACS buffer. 10^6 cells were stained for 20 minutes at room temperature with antibodies including FITC rat anti-mouse CD45, PE/Cy7 anti-mouse F4/80, PE anti-mouse CD11b, APC anti-mouse CD11c, Pacific Blue anti-mouse CD3, PE anti-mouse CD62L, PE anti-mouse Gr1, FITC anti-mouse Ly6C, Pacific blue anti-mouse CD86 (Bio-Legend), PE-Cy7 anti-mouse MHC class II (I-A/I-E) (eBiosciences), Alexa Fluor 647 (AbD Serotec), and anti-CX3CR1 (Abcam), then washed and resuspended in FACS buffer. After immunostaining, cells were analyzed immediately on a Facs Canto II cytometer with DIVA software (Becton Dickinson), and offline list mode data analysis was performed using Winlist software from Verity Software House. For Ki67 and BrdU staining, cell suspensions after F4/80 staining were incubated with Foxp3 Fixation/Permeabilization solution (catalog no. 00-5521; eBioscience) for 18 hours at 4°C in the dark, FACS buffer added, and centrifuged (800 g, 10 minutes, 8°C). The pellets were suspended in FACS buffer containing 1% normal mouse serum for 10 minutes on ice, PE mouse anti-human Ki67 or PE anti-BrdU (BioLegend) or isotype control (BD Biosciences — Pharmingen) added, and incubated (40 minutes, 4°C). The suspensions were washed twice with FACS buffer, resuspended in FACS buffer, and immediately analyzed.

Isolation of kidney monocytes/macrophages. CD11b^{hi} or CD11c$^+$ cells in kidney single-cell suspensions were enriched using mouse CD11b or CD11c Microbeads and MACS columns (Miltenyi Biotec) following the manufacturer's protocol.

PKH26 labeling and ex vivo polarization of splenic monocytes. Single spleen cell suspensions were prepared and enriched using mouse CD11b Microbeads and MACS columns. Bone marrow was harvested from BALB/c mice (for bilateral I/R injury) and B6D2 mice (for DT-induced injury), single-cell suspensions were prepared, and Ly6C$^+$ cells were enriched by negative selection with MACS columns according to methods described by Lin et al. (59). PKH26 red fluorescent cell linker kit for phagocytic cell labeling (Sigma-Aldrich) was used to label CD11b^{hi} splenic monocytes and bone marrow Ly6C$^+$ cells following the manufacturer's protocol. Each mouse received 2 × 10^6 PHK26-labeled splenic monocytes or 5 × 10^6 PHK26-labeled bone marrow Ly6C cells$^+$ via tail vein injection 4 hours before I/R or DT injection. For ex vivo polarization, we obtained macrophages by culturing splenic monocytes in RPMI 1640 medium for 48 hours (for M0 macrophages), in medium containing 2.5 μg/ml LPS for 2 hours and then an additional 46 hours in normal medium (for M1 macrophages), or in medium containing IL-4 and IL-13 (10 ng/ml each) for 48 hours (for M2 macrophages) (60). Each mouse received 5 × 10^5 polarized macrophages via tail vein injection 4 hours before DT injection or I/R. To investigate the infiltration of PKH26-labeled cells in the kidney, FPAS-perfused kidneys were immersed in 30% sucrose, cryosectioned, and then viewed and imaged with a Nikon TE300 fluorescence microscope.

RNA isolation and qRT-PCR. Total RNA from kidney or isolated macrophages was isolated using TRIzol reagents (Invitrogen). qRT-PCR was performed using TaqMan real-time PCR (7900HT; Applied Biosystems). The Master Mix and all gene probes were also purchased from Applied Biosystems. The probes used in the experiments included mouse *S18* (Mm02601778), *iNOS* (Mm00440502), *Il23a* (Mm00518984), *Ccl3* (Mm00441258), *Arg1* (Mm00475991), *Il4ra* (Mm01275139), *Igf2r* (Mm01329362), *Tgfb* (Mm00441726), and *Tnfa* (Mm99999068).

Measurement of serum BUN and creatinine and albuminuria. BUN was measured using a Urea Assay Kit (BioAssay Systems), and serum creatinine was measured by a previously described HPLC method (61). Either 24-hour urine collection or spot urine was obtained from individually caged mice using polycarbonate metabolic cages. Urinary albumin and creatinine excretion was determined using Albuwell-M kits (Exocell Inc.). Albuminuria for spot urine was determined as the ratio of urinary albumin (μg/ml) to creatinine (mg/ml).

Micrography. Brightfield images from a Leitz Orthoplan microscope with DVC digital RGB video camera were digitized and saved as computer files. Contrast and color level adjustment (Adobe Photoshop) were performed for the entire image; i.e., no region- or object-specific editing or enhancements were performed.

Statistics. Values are presented as mean ± SEM. ANOVA and Bonferroni 2-tailed t tests were used for statistical analysis, and differences were considered significant for P values less than 0.05.

Study approval. All animal experiments were performed in accordance with the guidelines of the Institutional Animal Care and Use Committee of Vanderbilt University.

Acknowledgments

Address correspondence to: Raymond C. Harris, Division of Nephrology, C3121 MCN, Vanderbilt University School of Medicine and Nashville Veterans Affairs Hospital, Nashville, Tennessee 37232, USA. Phone: 615.322.2150; Fax: 615.343.2675; E-mail: ray.harris@vanderbilt.edu. Or to: Ming-Zhi Zhang, S-3206 MCN, Vanderbilt University Medical Center, Nashville, Tennessee 37232, USA. Phone: 615.343.1548; Fax: 615.343.2675; E-mail: ming-zhi.zhang@vanderbilt.edu.

1. Devarajan P. Emerging biomarkers of acute kidney injury. *Expert Opin Med Diagn.* 2008;2(4):387–398.
2. Bajwa A, Kinsey GR, Okusa MD. Immune mechanisms and novel pharmacological therapies of acute kidney injury. *Curr Drug Targets.* 2009;10(12):1196–1204.
3. Kelly KJ, et al. Intercellular adhesion molecule-1-deficient mice are protected against ischemic renal injury. *J Clin Invest.* 1996;97(4):1056–1063.
4. Kelly KJ, Meehan SM, Colvin RB, Williams WW, Bonventre JV. Protection from toxicant-mediated renal injury in the rat with anti-CD54 antibody. *Kidney Int.* 1999;56(3):922–931.
5. Day YJ, Huang L, Ye H, Li L, Linden J, Okusa MD. Renal ischemia-reperfusion injury and adenosine 2A receptor-mediated tissue protection: the role of CD4+ T cells and IFN-gamma. *J Immunol.* 2006;176(5):3108–3114.
6. Burne MJ, et al. Identification of the CD4(+) T cell as a major pathogenic factor in ischemic acute renal failure. *J Clin Invest.* 2001;108(9):1283–1290.
7. Day YJ, Huang L, Ye H, Linden J, Okusa MD. Renal ischemia-reperfusion injury and adenosine 2A receptor-mediated tissue protection: role of macrophages. *Am J Physiol Renal Physiol.* 2005;288(4):F722–F731.
8. Oh DJ, et al. Fractalkine receptor (CX3CR1) inhibition is protective against ischemic acute renal failure in mice. *Am J Physiol Renal Physiol.* 2008;294(1):F264–F271.
9. Jo SK, Sung SA, Cho WY, Go KJ, Kim HK. Macrophages contribute to the initiation of ischaemic acute renal failure in rats. *Nephrol Dial Transplant.* 2006;21(5):1231–1239.
10. Cantaluppi V, et al. Macrophage stimulating protein may promote tubular regeneration after acute injury. *J Am Soc Nephrol.* 2008;19(10):1904–1918.
11. Humphreys BD, et al. Intrinsic epithelial cells repair the kidney after injury. *Cell Stem Cell.* 2008;2(3):284–291.
12. Al-Awqati Q, Oliver JA. The kidney papilla is a stem cells niche. *Stem Cell Rev.* 2006;2(3):181–184.
13. Langworthy M, Zhou B, de Caestecker M, Moeckel G, Baldwin HS. NFATc1 identifies a population of proximal tubule cell progenitors. *J Am Soc Nephrol.* 2009;20(2):311–321.
14. Appel D, et al. Recruitment of podocytes from glomerular parietal epithelial cells. *J Am Soc Nephrol.* 2009;20(2):333–343.

15. Harris RC. Growth factors and cytokines in acute renal failure. *Adv Ren Replace Ther*. 1997; 4(2 suppl 1):43–53.

16. Zeng F, Singh AB, Harris RC. The role of the EGF family of ligands and receptors in renal development, physiology and pathophysiology. *Exp Cell Res*. 2009;315(4):602–610.

17. Guo JK, Cantley LG. Cellular maintenance and repair of the kidney. *Annu Rev Physiol*. 2010;72:357–376.

18. Benoit M, Desnues B, Mege JL. Macrophage polarization in bacterial infections. *J Immunol*. 2008; 181(6):3733–3739.

19. Rees AJ. Monocyte and macrophage biology: an overview. *Semin Nephrol*. 2010;30(3):216–233.

20. Hume DA. Macrophages as APC and the dendritic cell myth. *J Immunol*. 2008;181(9):5829–5835.

21. Duffield JS, et al. Selective depletion of macrophages reveals distinct, opposing roles during liver injury and repair. *J Clin Invest*. 2005;115(1):56–65.

22. Arnold L, et al. Inflammatory monocytes recruited after skeletal muscle injury switch into antiinflammatory macrophages to support myogenesis. *J Exp Med*. 2007;204(5):1057–1069.

23. Nahrendorf M, et al. The healing myocardium sequentially mobilizes two monocyte subsets with divergent and complementary functions. *J Exp Med*. 2007;204(12):3037–3047.

24. Lee S, et al. Distinct macrophage phenotypes contribute to kidney injury and repair. *J Am Soc Nephrol*. 2011;22(2):317–326.

25. Nelson PJ, Rees AJ, Griffin MD, Hughes J, Kurts C, Duffield J. The renal mononuclear phagocytic system. *J Am Soc Nephrol*. 2012;23(2):194–203.

26. Schaffner DL, et al. Targeting of the rasT24 oncogene to the proximal convoluted tubules in transgenic mice results in hyperplasia and polycystic kidneys. *Am J Pathol*. 1993;142(4):1051–1060.

27. Li L, et al. The chemokine receptors CCR2 and CX3CR1 mediate monocyte/macrophage trafficking in kidney ischemia-reperfusion injury. *Kidney Int*. 2008;74(12):1526–1537.

28. Menke J, et al. CSF-1 signals directly to renal tubular epithelial cells to mediate repair in mice. *J Clin Invest*. 2009;119(8):2330–2342.

29. Conway JG, et al. Effects of the cFMS kinase inhibitor 5-(3-methoxy-4-((4-methoxybenzyl)oxy)benzyl)pyrimidine-2,4-diamine (GW2580) in normal and arthritic rats. *J Pharmacol Exp Ther*. 2008;326(1):41–50.

30. Kielar ML, et al. Maladaptive role of IL-6 in ischemic acute renal failure. *J Am Soc Nephrol*. 2005; 16(11):3315–3325.

31. Kinsey GR, Li L, Okusa MD. Inflammation in acute kidney injury. *Nephron Exp Nephrol*. 2008; 109(4):e102–e107.

32. Takada M, Nadeau KC, Shaw GD, Marquette KA, Tilney NL. The cytokine-adhesion molecule cascade in ischemia/reperfusion injury of the rat kidney. Inhibition by a soluble P-selectin ligand. *J Clin Invest*. 1997;99(11):2682–2690.

33. Bonventre JV, Zuk A. Ischemic acute renal failure: an inflammatory disease? *Kidney Int*. 2004; 66(2):480–485.

34. He Z, Dursun B, Oh DJ, Lu L, Faubel S, Edelstein CL. Macrophages are not the source of injurious interleukin-18 in ischemic acute kidney injury in mice. *Am J Physiol Renal Physiol*. 2009;296(3):F535–F542.

35. Furuichi K, et al. Gene therapy expressing aminoterminal truncated monocyte chemoattractant protein-1 prevents renal ischemia-reperfusion injury. *J Am Soc Nephrol*. 2003;14(4):1066–1071.

36. Danenberg HD, et al. Macrophage depletion by clodronate-containing liposomes reduces neointimal formation after balloon injury in rats and rabbits. *Circulation*. 2002;106(5):599–605.

37. Zhao M, et al. Alveolar macrophage activation is a key initiation signal for acute lung ischemia-reperfusion injury. *Am J Physiol Lung Cell Mol Physiol*. 2006;291(5):L1018–L1026.

38. Tagliani E, Shi C, Nancy P, Tay CS, Pamer EG, Erlebacher A. Coordinate regulation of tissue macrophage and dendritic cell population dynamics by CSF-1. *J Exp Med*. 2011;208(9):1901–1916.

39. Werner S, Grose R. Regulation of wound healing by growth factors and cytokines. *Physiol Rev*. 2003; 83(3):835–870.

40. Ricardo SD, van Goor H, Eddy AA. Macrophage diversity in renal injury and repair. *J Clin Invest*. 2008; 118(11):3522–3530.

41. Lin SL, et al. Macrophage Wnt7b is critical for kidney repair and regeneration. *Proc Natl Acad Sci U S A*. 2010;107(9):4194–4199.

42. Nagata S, Hanayama R, Kawane K. Autoimmunity and the clearance of dead cells. *Cell*. 2010; 140(5):619–630.

43. Freire-de-Lima CG, Xiao YQ, Gardai SJ, Bratton DL, Schiemann WP, Henson PM. Apoptotic cells, through transforming growth factor-beta, coordinately induce anti-inflammatory and suppress pro-inflammatory eicosanoid and NO synthesis in murine macrophages. *J Biol Chem*. 2006; 281(50):38376–38384.

44. Jenkins SJ, et al. Local macrophage proliferation, rather than recruitment from the blood, is a signature of TH2 inflammation. *Science*. 2011; 332(6035):1284–1288.

45. Pollard JW. Trophic macrophages in development and disease. *Nature Rev Immunol*. 2009;9(4):259–270.

46. Gordon S, Martinez FO. Alternative activation of macrophages: mechanism and functions. *Immunity*. 2010;32(5):593–604.

47. Edwards JP, Zhang X, Mosser DM. The expression of heparin-binding epidermal growth factor-like growth factor by regulatory macrophages. *J Immunol*. 2009;182(4):1929–1939.

48. Fadok VA, Bratton DL, Guthrie L, Henson PM. Differential effects of apoptotic versus lysed cells on macrophage production of cytokines: role of proteases. *J Immunol*. 2001;166(11):6847–6854.

49. Geissmann F, Gordon S, Hume DA, Mowat AM, Randolph GJ. Unravelling mononuclear phagocyte heterogeneity. *Nat Rev Immunol*. 2010;10(6):453–460.

50. Kruger T, et al. Identification and functional characterization of dendritic cells in the healthy murine kidney and in experimental glomerulonephritis. *J Am Soc Nephrol*. 2004;15(3):613–621.

51. Mosser DM, Edwards JP. Exploring the full spectrum of macrophage activation. *Nat Rev Immunol*. 2008; 8(12):958–969.

52. Terzi F, et al. Targeted expression of a dominant-negative EGF-R in the kidney reduces tubulo-interstitial lesions after renal injury. *J Clin Invest*. 2000; 106(2):225–234.

53. Iwano M, Plieth D, Danoff TM, Xue C, Okada H, Neilson EG. Evidence that fibroblasts derive from epithelium during tissue fibrosis. *J Clin Invest*. 2002; 110(3):341–350.

54. Mitamura T, Higashiyama S, Taniguchi N, Klagsbrun M, Mekada E. Diphtheria toxin binds to the epidermal growth factor (EGF)-like domain of human heparin-binding EGF-like growth factor/diphtheria toxin receptor and inhibits specifically its mitogenic activity. *J Biol Chem*. 1995; 270(3):1015–1019.

55. Zhang MZ, Yao B, Cheng HF, Wang SW, Inagami T, Harris RC. Renal cortical cyclooxygenase 2 expression is differentially regulated by angiotensin II AT(1) and AT(2) receptors. *Proc Natl Acad Sci U S A*. 2006;103(43):16045–16050.

56. Zhang MZ, Yao B, Fang X, Wang S, Smith JP, Harris RC. Intrarenal dopaminergic system regulates renin expression. *Hypertension*. 2009;53(3):564–570.

57. Wang Z, Chen JK, Wang SW, Moeckel G, Harris RC. Importance of functional EGF receptors in recovery from acute nephrotoxic injury. *J Am Soc Nephrol*. 2003;14(12):3147–3154.

58. Harris RC, McKanna JA, Akai Y, Jacobson HR, Dubois RN, Breyer MD. Cyclooxygenase-2 is associated with the macula densa of rat kidney and increases with salt restriction. *J Clin Invest*. 1994; 94(6):2504–2510.

59. Lin SL, Castaño AP, Nowlin BT, Lupher ML Jr, Duffield JS. Bone marrow Ly6Chigh monocytes are selectively recruited to injured kidney and differentiate into functionally distinct populations. *J Immunol*. 2009;183(10):6733–6743.

60. Wang Y, et al. Ex vivo programmed macrophages ameliorate experimental chronic inflammatory renal disease. *Kidney Int*. 2007;72(3):290–299.

61. Zhao HJ, et al. Endothelial nitric oxide synthase deficiency produces accelerated nephropathy in diabetic mice. *J Am Soc Nephrol*. 2006;17(10):2664–2669.